# Supplementary Information

Stable and efficient n = 2 Ruddlesden-Popper La/Pr nickelates as oxygen electrodes for SOCs applications

Romuald Frugier[a], Jacinthe Gamon[a], Sébastien Fourcade[a], Sonia Buffière[a], Jean-Marc Bassat[a,*]

[a] *CNRS, Univ. Bordeaux, Bordeaux INP, ICMCB, UMR 5026, F-33600 PESSAC Cedex, France*

* corresponding author : jean-marc.bassat@icmcb.cnrs.fr
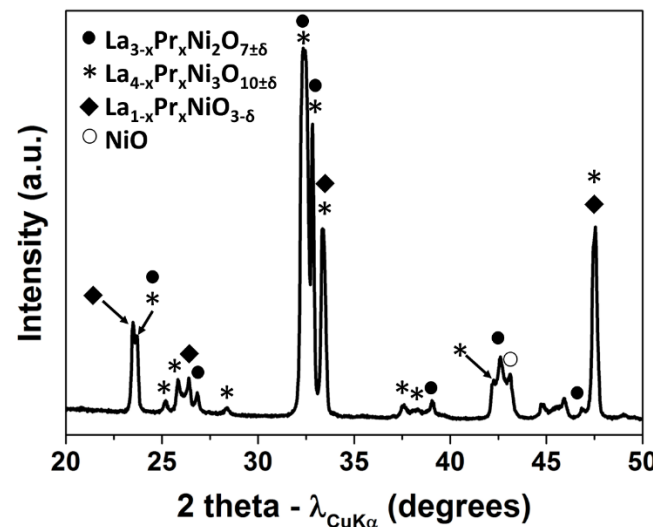
Fig. S1 Powder XRD diagram for $La_{1.125}Pr_{1.875}Ni_2O_{7\pm\delta}$ synthesis under O_2 gas flow at 1150 °C for 120 h
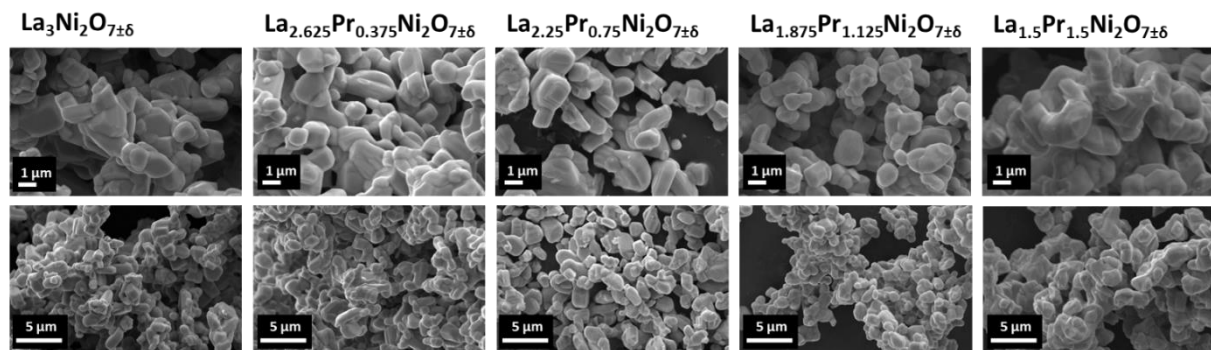
**Fig. S2** SEM pictures of the as-prepared powder of $La_{3-x}Pr_xNi_2O_{7\pm\delta}$ ($x \leq 1.5$)
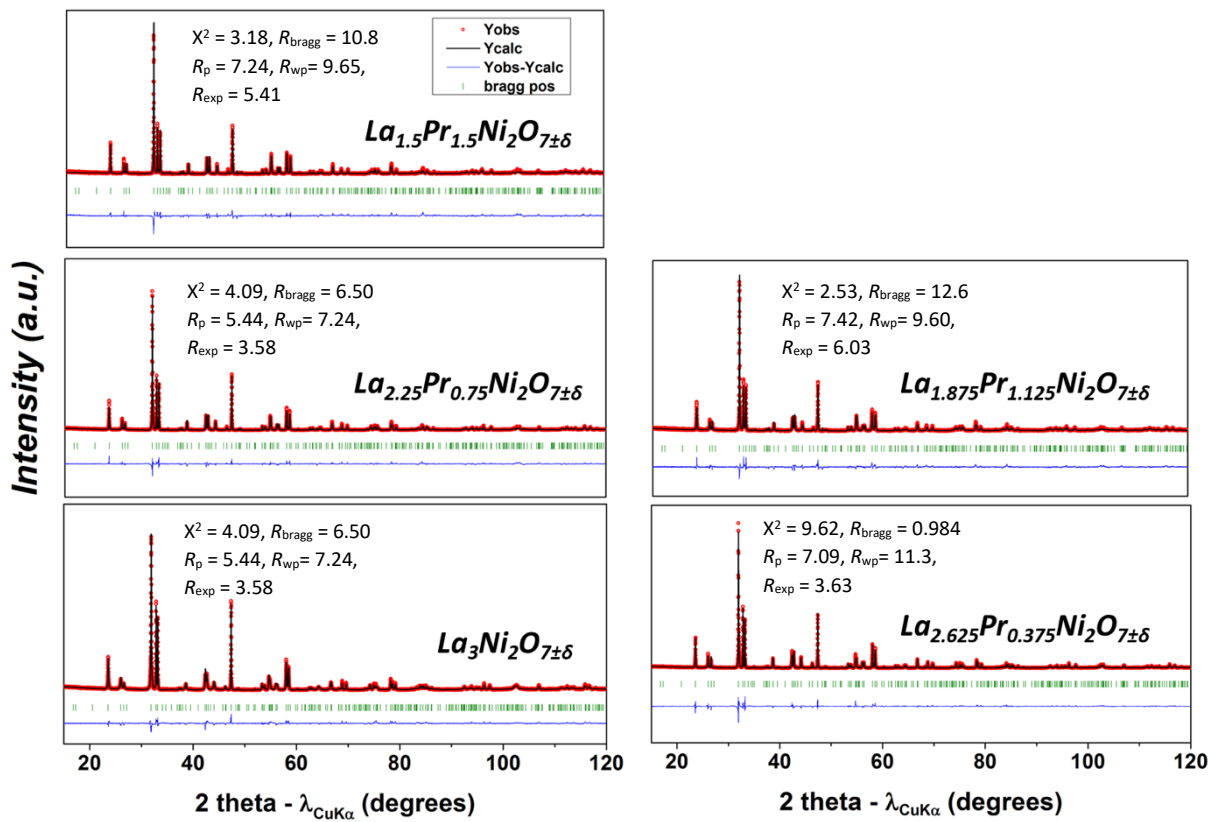
Fig. S3 Rietveld refinement patterns for $La_{3-x}Pr_xNi_2O_{7\pm\delta}$ with x = 0, 0.375, 0.75, 1.125, 1.5.
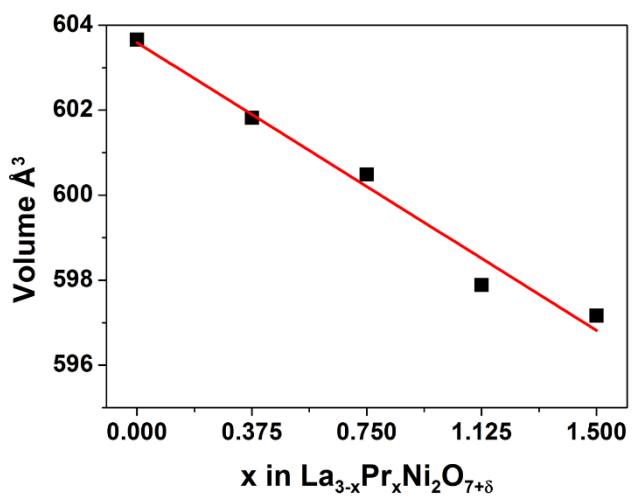
Fig. S4 Cell volume evolution in function of *x* in $La_{3-x}Pr_xNi_2O_{7\pm\delta}$ from Rietveld refinement
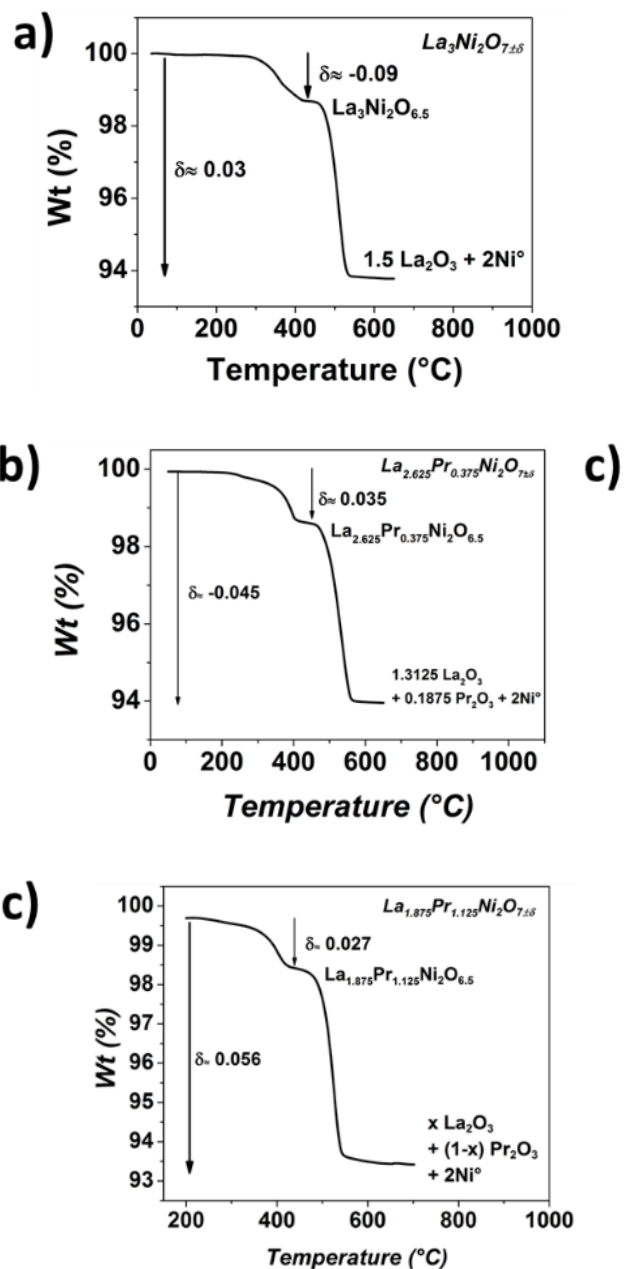
Fig. S5 TGA plot under Ar-5 % H_2, a) $x = 0$, b) $x = 0.375$, c) $x = 1.125$

Table S1 Structural parameters for the different $n = 2$ Ruddlesden-Popper nickelates determined by Rietveld refinements with the orthorhombic *Amam* space group. Standard variations were multiplied by the Berar factor (4.6, 4.0, 3.7, 3.8, 5.2, for $x = 0$, 0.375, 0.75, 1.125, 1.5 respectively).

Large standard variations were obtained for the isotropic displacement , B, due to the difficulty of correct modelling of the peak shapes. This was attributed to the presence of structural defects, such as stacking faults, to which RP phases are often subjected. The B value for atoms of the same type (equatorial oxygen O3 and O4 as well as the two *Ln* sites) were constraint to the same value.

La₃Ni₂O₇±δ, *a* = 5.39744(9) Å, *b* = 5.44944(2) Å, *c* = 20.5219(6) Å

Atom	X	Y	Z	B (Å)	Occupancy	Wyckoff site
La1	0.25	0.245(5)	0.5	0.16(6)	1	4c
La2	0.25	0.256(3)	0.3189(2)	0.16(6)	1	8g
Ni1	0.25	0.252(11)	0.0984(6)	0.56(22)	1	8g
O1	0.25	0.295(28)	0	2(2)	1	4c
O2	0.25	0.283(26)	0.2027(27)	4(2)	1	8g
O3	0	0.5	0.1071(36)	1.5(9)	1	8e
O4	0.5	0	0.0822(38)	1.5(9)	1	8e

La₂.₆₂₅Pr₀.₃₇₅Ni₂O₇±δ, *a* = 5.3871(4) Å, *b* = 5.45187(4) Å, *c* = 20.4871(3) Å

Atom	X	Y	Z	B (Å)	Occupancy	Wyckoff site
La1	0.25	0.249(4)	0.5	0.04(4)	0.875	4c
Pr1	0.25	0.249(4)	0.5	0.04(4)	0.125	4c
La2	0.25	0.255(3)	0.31924(16)	0.04(4)	0.875	8g
Pr2	0.25	0.255(3)	0.31924(16)	0.04(4)	0.125	8g
Ni1	0.25	0.254(8)	0.09841(16)	0.16(16)	1	8g
O1	0.25	0.258(8)	0	6(2)	1	4c
O2	0.25	0.22(2)	0.202(2)	1.7(12)	1	8g
O3	0	0.5	0.1064(24)	0.15(16)	1	8e
O4	0.5	0	0.0812(28)	0.15(16)	1	8e

La₂.₂₅Pr₀.₇₅Ni₂O₇±δ, *a* = 5.3841(1) Å, *b* = 5.4550(1) Å, *c* = 20.4478(5) Å

Atom	X	Y	Z	B (Å)	Occupancy	Wyckoff site
La1	0.25	0.248(4)	0.5	0.145(41)	0.75	4c
Pr1	0.25	0.248(4)	0.5	0.145(41)	0.25	4c
La2	0.25	0.251(6)	0.3203(2)	0.145(41)	0.75	8g
Pr2	0.25	0.251(6)	0.3203(2)	0.145(41)	0.25	8g
Ni1	0.25	0.250(9)	0.1088(3)	0.235(155)	1	8g
O1	0.25	0.30(1)	0	4.3(24)	1	4c
O2	0.25	0.23(2)	0.212(2)	3(1)	1	8g
O3	0	0.5	0.106(3)	1.0(7)	1	8e
O4	0.5	0	0.069(3)	1.0(7)	1	8e

La₁.₈₇₅Pr₁.₁₂₅Ni₂O₇±δ, *a* = 5.3774(1) Å, *b* = 5.4551(1) Å, *c* = 20.3886(6) Å

Atom	X	Y	Z	B (Å)	Occupancy	Wyckoff site
La1	0.25	0.2502(45)	0.5	0.804(15)	0.375	4c
Pr1	0.25	0.2502(45)	0.5	0.804(15)	0.625	4c
La2	0.25	0.255(3)	0.3197(3)	0.23(8)	0.375	8g
Pr2	0.25	0.255(3)	0.3197(3)	0.23(8)	0.625	8g
Ni1	0.25	0.257(4)	0.1098(4)	0.41(21)	1	8g
O1	0.25	0.324(17)	0	2(2)	1	4c
O2	0.25	0.22(18)	0.215(3)	2.2 (12)	1	8g
O3	0	0.5	0.108(3)	2.0 (12)	1	8e
O4	0.5	0	0.073(3)	2.0 (12)	1	8e

La₁.₅Pr₁.₅Ni₂O₇±δ, *a* = 5.3718(6) Å, *b* = 5.4594(5) Å, *c* = 20.362(3) Å

Atom	X	Y	Z	B (Å)	Occupancy	Wyckoff site
La1	0.25	0.25(1)	0	0.73(5)	0.5	4c
Pr1	0.25	0.25(1)	0.5	0.73(5)	0.5	4c
La2	0.25	0.255(5)	0.319(25)	0.73(5)	0.5	8g
Pr2	0.25	0.255(5)	0.319(25)	0.73(5)	0.5	8g
Ni1	0.25	0.25(2000)	0.0969(5)	1.23(35)	1	8g
O1	0.25	0.30(3)	0	1.4(30)	1	4c
O2	0.25	0.20(2)	0.204(3)	1.5(20)	1	8g
O3	0	0.5	0.108(4)	0.5(10)	1	8e
O4	0.5	0	0.085(5)	0.5(10)	1	8e
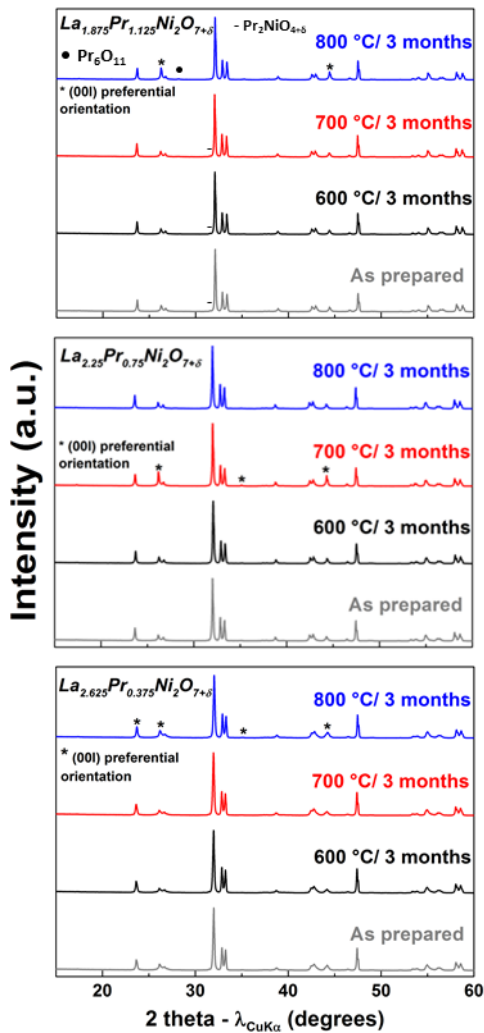
Fig. S6 Diffractograms of La$_{2.625}$Pr$_{0.375}$Ni$_2$O$_{7\pm\delta}$, La$_{2.25}$Pr$_{0.75}$Ni$_2$O$_{7\pm\delta}$ and La$_{1.875}$Pr$_{1.125}$Ni$_2$O$_{7\pm\delta}$ aged at 600, 700 and 800 °C for 3 months and as-prepared. * These (00*l*) reflections are subject to preferential orientation. The presence of Pr$_6$O$_{11}$ in La$_{1.875}$Pr$_{1.125}$Ni$_2$O$_{7\pm\delta}$ aged at 800 °C for 3 months comes from the decomposition of the small Pr$_2$NiO$_{4+\delta}$ impurity obtained after synthesis due to a slight deviation from the exact stoichiometry when weighting the precursors
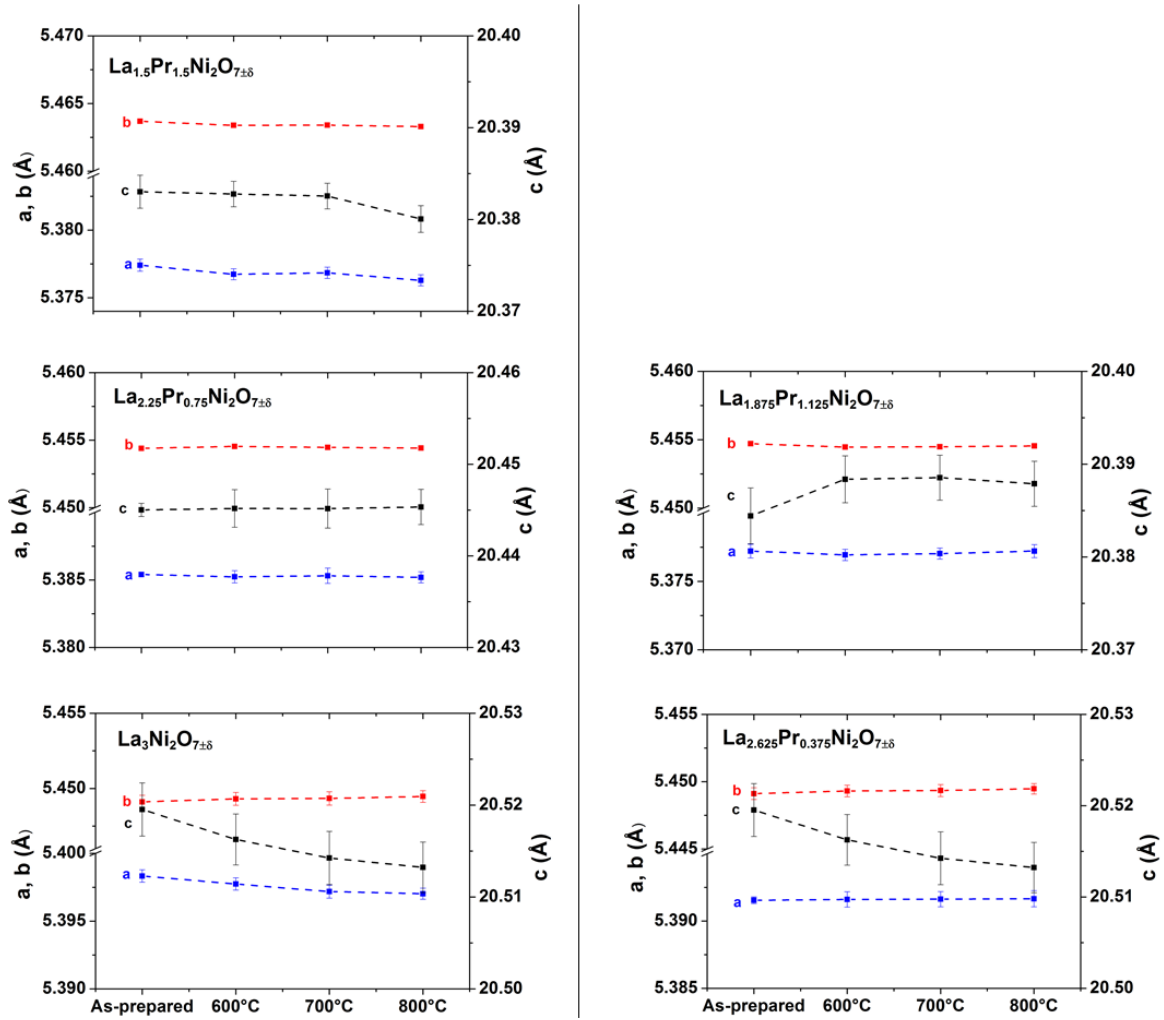
Fig. S7 Cell parameters obtained through profile matching refinement against the data of $La_{3-x}Pr_xNi_2O_{7\pm\delta}$ aged at 600, 700 and 800°C for 1 month and as-prepared
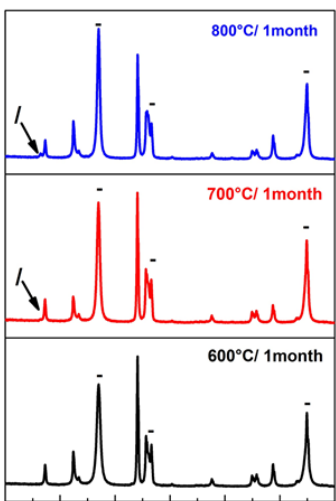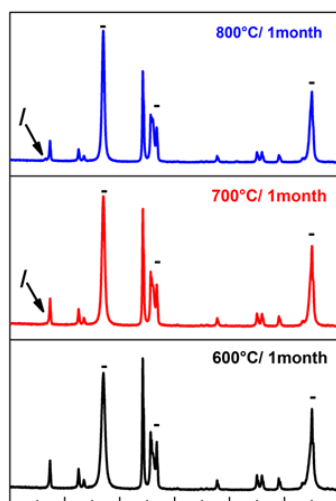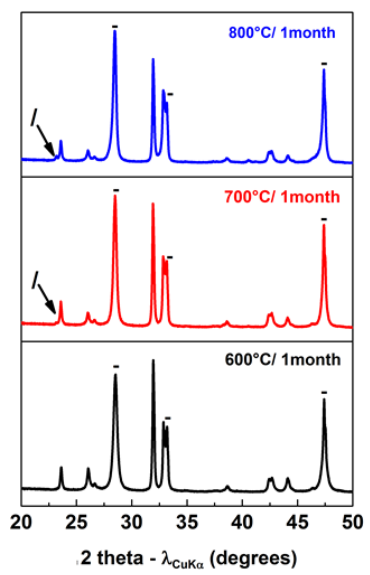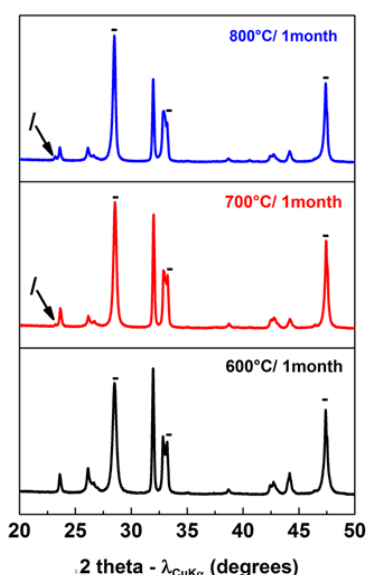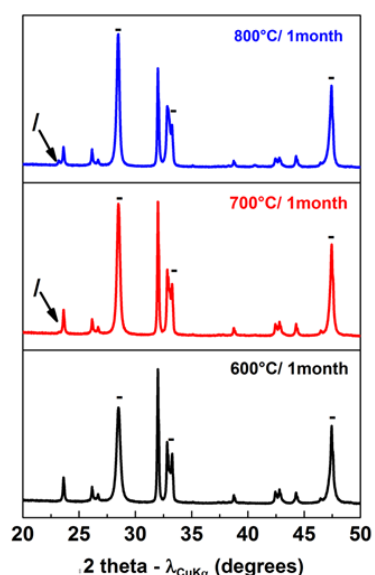
**Fig S8** Diffractogram (20-60°) of the aged GDC/ $La_3Ni_2O_{7\pm\delta}$ mixture at 800 °C for 1 month. / corresponds to the $La_{1-x}Pr_xNiO_{3-\delta}$ perovskite phase, - to GDC and unlabelled peaks the $La_{3-x}Pr_xNi_2O_{7\pm\delta}$ phase
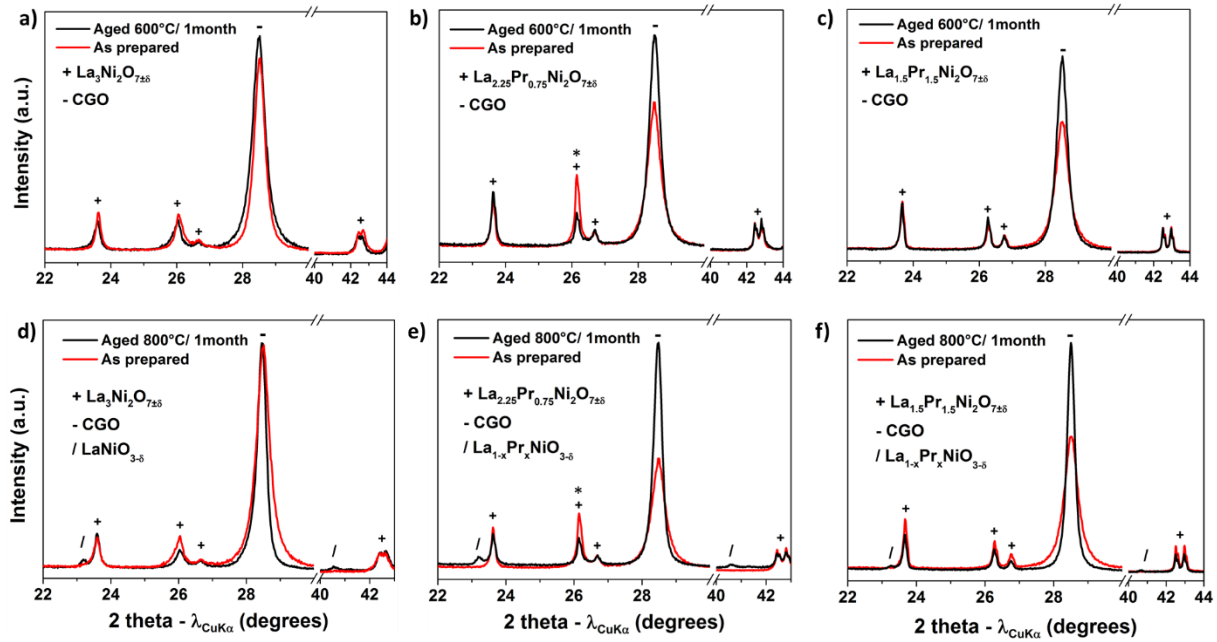
Fig. S9 Powder XRD diagrams (zooms) of the nickelate and GDC mixture as-prepared and after ageing at 600 °C and 800 °C for 1 month for (a, d) $La_3Ni_2O_{7\pm\delta}$, (b, e) $La_{2.25}Pr_{0.75}Ni_2O_{7\pm\delta}$ and, (c, f) $La_{1.5}Pr_{1.5}Ni_2O_{7\pm\delta}$. * These (00$l$) reflections are subject to preferential orientation
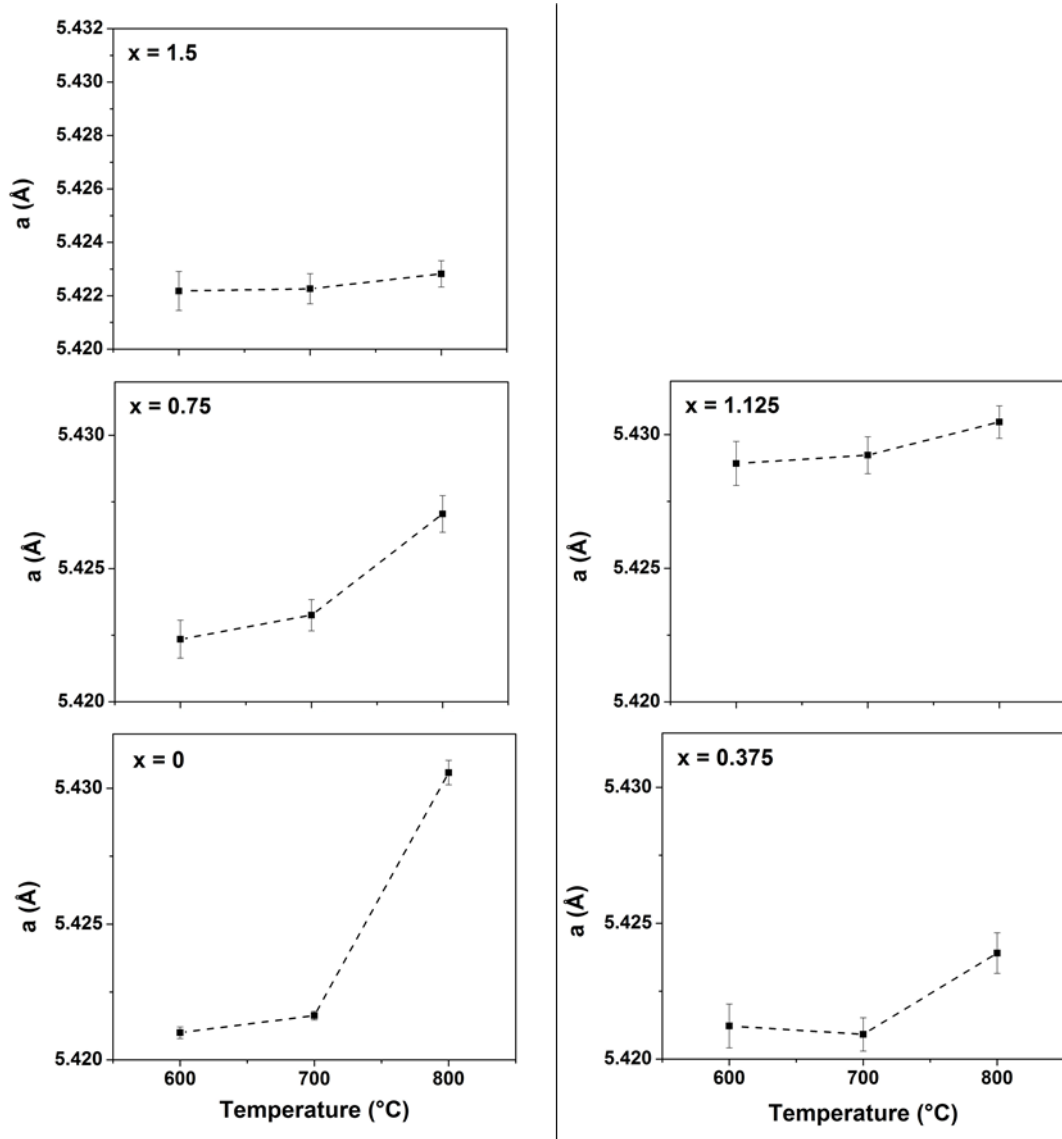
Fig. S10 Cell parameters of the GDC phase obtained through profile matching refinement against the XRD data of GDC aged in presence of $La_{3-x}Pr_xNi_2O_{7\pm\delta}$ at 600, 700 and 800 °C for 1 month and as-prepared.
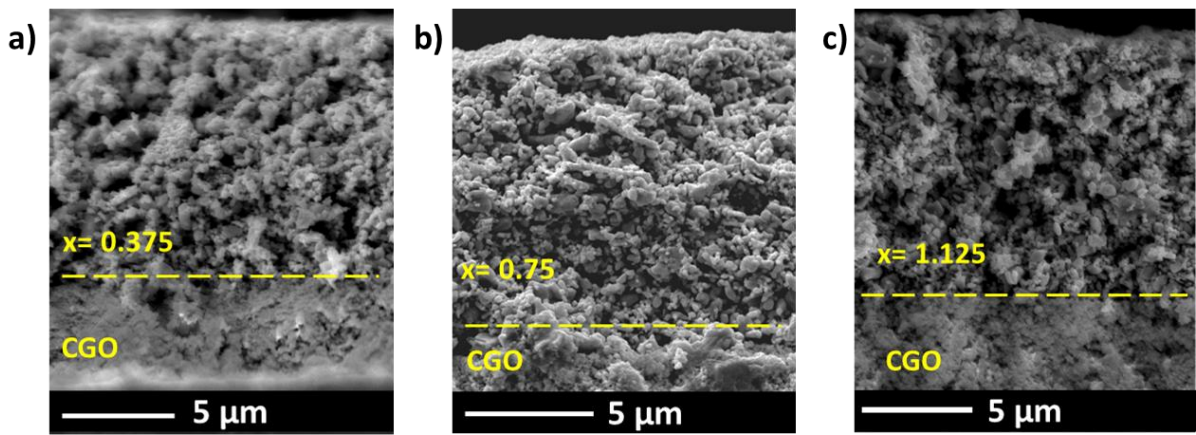
Fig. S11 SEM images of the symmetrical cells of (a) $La_{2.625}Pr_{0.375}Ni_2O_{7\pm\delta}$,(b) $La_{2.25}Pr_{0.75}Ni_2O_{7\pm\delta}$ and, (c) $La_{1.875}Pr_{1.125}Ni_2O_{7\pm\delta}$. All pictures were taken with a magnification of 5000.

Table S2 Parameters used to fit the Nyquist obtained at 600°C. Standard uncertainties are those given by the fitting which are largely underestimated.

	$La_3Ni_2O_{7\pm\delta}$	$La_{2.625}Pr_{0.375}Ni_2O_{7\pm\delta}$	$La_{2.25}Pr_{0.75}Ni_2O_{7\pm\delta}$	$La_{1.875}Pr_{1.125}Ni_2O_{7\pm\delta}$	$La_{1.5}Pr_{1.5}Ni_2O_{7\pm\delta}$
R_s ($\Omega.cm^2$)	2.829 ± 0.001	4.538 ± 0.007	2.8503 ± 0.0005	4.7941 ± 0.0002	3.5412 ± 0.0004
R_1 ($\Omega.cm^2$)	1.760 ± 0.002	0.242 ± 0.001	0.2389 ± 0.0007	0.2238 ± 0.0002	0.4430 ± 0.0005
Q_1 ($S.s^n$)	0.001331 ± 0.000003	0.000232 ± 0.000001	0.0067 ± 0.0001	0.0188 ± 0.0001	0.00470 ± 0.00002
n_1	0.5638 ± 0.0002	0.947 ± 0.002	0.627 ± 0.001	0.5525 ± 0.0004	0.8357 ± 0.0006
R_2 ($\Omega.cm^2$)	2.043± 0.002	1.380 ± 0.002	1.220 ± 0.001	0.4583 ± 0.0002	
Q_1 ($S.s^n$)	0.001488 ± 0.000004	0.00142 ± 0.00001	0.00229 ± 0.00001	0.001155 ± 0.000002	
n_2	0.7803 ± 0.0004	0.7556 ± 0.0004	0.8098 ± 0.0003	0.9617 ± 0.0002	
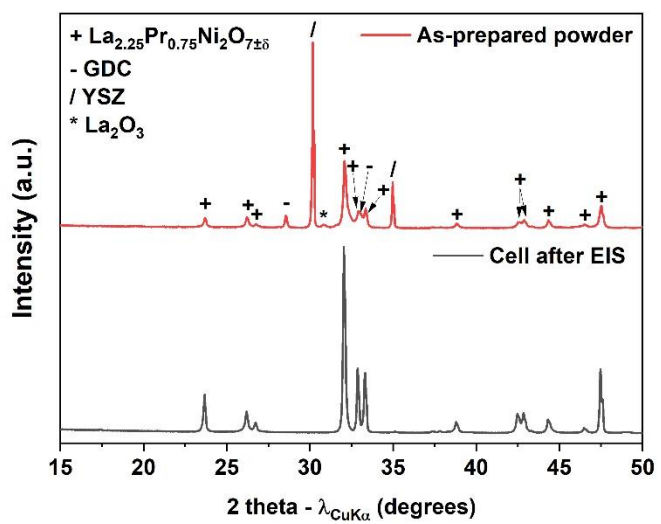
Fig. S12 XRD diagram of the as-prepared $La_{2.25}Pr_{0.75}Ni_2O_{7\pm\delta}$// GDC// YSZ symmetrical cell, co-sintered at 950 °C for 2 h.
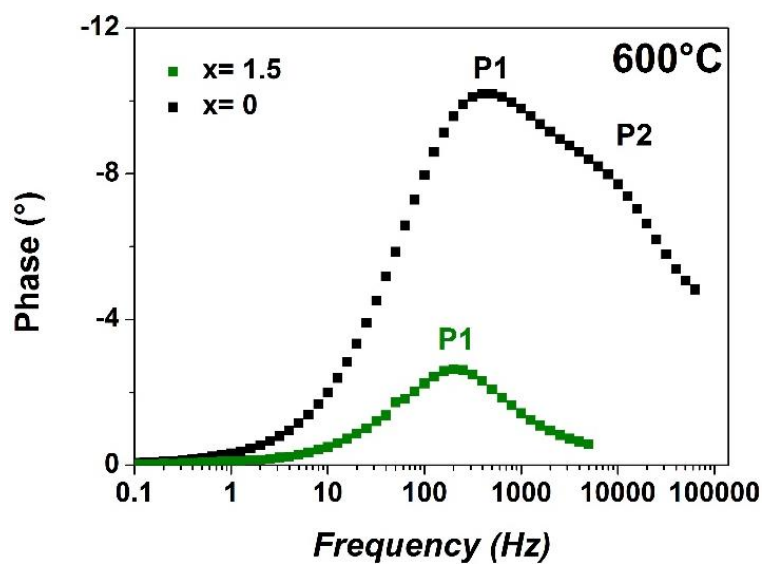
Fig. S13 Bode plot of $La_3Ni_2O_{7\pm\delta}$ and $La_{1.5}Pr_{1.5}Ni_2O_{7\pm\delta}$ obtained at 600°C.